International Journal of Composite Materials 2016, 6(3): 68-78
DOI: 10.5923/j.cmaterials.20160603.02

Parametric Study of Tri-axially Braided Composites

Mohamad Ismail, Ali Ismail, Mohammad Hammoud, Ali Hallal*

Mechanical Department, School of Engineering, Lebanese International University, Beirut, Lebanon

Abstract In this paper, a parametric study of mechanical properties for tri-axially braided composite is presented. The main parameters involved are: the braid angle "θ", the fiber volume fraction "V_f" and the fiber type. An analytical modeling is adopted to evaluate the 3D elastic properties and ultimate strengths. This model is based on a multi-scale homogenization method, the 3SHM (three Stages Homogenization Method) where Tsai-Wu and Christensen Failure criteria and a damaged stiffness model are used to predict the failure of composites. A validation of the analytical model is done by comparing the results with available experimental and numerical FE data. At the braid angle θ = 50°, and for different types of fibers and V_f, the composite is almost in-plane isotropic, where in-plane Young's moduli and tensile strengths are equal. At this angle, the highest values of the in-plane shear modulus and shear strength are obtained.

Keywords Fabrics, Textiles, Mechanical properties, Strength, Analytical modelling

1. Introduction

Composites materials, and especially textiles, are taken more attention due to their mechanical properties. This paper presents a parametric study of the mechanical properties for a particular type of textile composites, the 2D tri-axially braided composite. As known, these types of fabrics are characterized by their braid angle and composed from two braided yarns and one axial yarn. Braided yarns make an angle that varies between zero and ninety degree; the common angles are 30, 45 and 60 degrees. Thus, a variety of braided composite architectures are found taking into account that different fiber volume fraction and fiber types can also be involved. The variation of these parameters leads to different mechanical properties of the material.

The prediction of elastic properties and ultimate strengths of textile composites has been done using analytical and numerical Finite Element models. In Literature most of the studies focus on woven composites, plain weave, satin and Twill fabrics, however less studies are found for the braided fabrics. Byun et al. [1] studied a two-step braided composite by two analytical models: a micro-cell model and a macro-cell model. The micro-cell model presents an attempt to combine the iso-strain and iso-stress assumptions in assembling different laminates composing the REV (Representative Elementary Volume) using CLT (Classical Laminates Theory). At first, an iso-stress assumption is used along the axial direction and then, iso-strain assumption is used along the transverse direction. The macro cell model represents a volume averaging model using iso-strain assumption. Results for in-plane elastic properties compared to those experimental reveal that micro cell model yields better results for axial Young's modulus and the in-plane Poisson's ratio, while both models yield less accurate results for the axial shear modulus.

A 3D iso-strain model is presented by Shokrieh and Mazloomi [2] to evaluate the stiffness of tri-axially braided composite. In this model, the composite is treated as a set of several layers representing braided and axial yarns. The stiffness of sinusoidal off-axis braided layers and axial layers are estimated using the layers fiber volume fraction equal to that of the REV. Then, the stiffness of the REV is obtained from averaging the stiffness matrices of the layers over their thickness fractions. They compared their results to those obtained from a stiffness "volume averaging" model and experimental data presented by Quek et al. [3]. Results show improvements in the prediction of the transverse Young's modulus "E_y" and the in-plane shear modulus "G_{xy}". Numerical finite element modeling is done for 3D tri-axially braided composites. Almost a good agreement is found for Young's moduli while less agreement is found for axial shear modulus [4]. Fewer studies are found concerning the prediction of ultimate strengths [5-8]. Li [9] used the iso-strain model form modeling 3D braided composites. A good agreement with experimental results for axial Young's modulus and tensile strength with an error not exceeding 10% when applied on 3D five directional braided composites. More recently, Jiang et al. [10] proposed a geometrical modeling, the helix model, and used the iso-strain model and Tsai-Wu failure criterion in order to evaluate the elastic properties and ultimate strengths of 3D braided composites. Axial Young's

* Corresponding author:
ali.hallal@liu.edu.lb (Ali Hallal)
Published online at http://journal.sapub.org/cmaterials

modulus and ultimate strength are compared to experimental data where good agreement is shown.

The main objective of this study is to investigate the influence on mechanical properties of braid angles, fiber volume fraction and the fiber type. Such kind of parametric study is beneficial for any engineer and designer that would use the optimum braided architecture for his design. It enables the selection of the appropriate braid angle, fiber volume fraction and fiber types that could fit the design requirements and tends to save the maximum weight. In the case of this study, the large number of investigated braided composites with their different architectures conducting to eliminate the experimental tests and numerical Finite Element modeling as a tool for evaluating mechanical properties. Moreover, the desired mechanical properties comports the all three dimensional properties, in-plane and out of plane properties, which makes the experimental and numerical evaluations almost impossible. Experimental tests will be very expensive in terms of money and time, while available numerical modeling will be time dependent and can't afford all needed properties especially concerning ultimate strengths. Thus, an analytical modeling of the mechanical properties is adopted. The presented analytical model is originally developed and yet used for woven composites [11, 12].

2. Modeling

The analytical model which provides the 3D elastic properties, ultimate strengths and the stress-strain diagrams for axial and shear loadings, is presented. The proposed analytical modeling is composed from a homogenization method, failure criteria and a damaged stiffness model as shown in Figure 1. A geometrical modeling relying on a sinusoidal modeling of the undulated yarns is adopted. Chamis micromechanical model [13, 14] is used to determine the elastic properties and ultimate strengths of subdivisions-UD composites. Then the analytical homogenization method developed by [11, 12] tends to predict the stiffness matrix of the composite and to evaluate the stress-strain fields throughout the composite. The fourth component of this model is the failure criteria, which is the Tsai-Wu failure criterion. The fifth component used is a damaged stiffness model for subdivisions-UD composites as shown in Figure 1.

The proposed failure prediction algorithm as shown in "Figure 1" tries to predict the failure of the composite based on the following conditions:

1. Final failure is assumed when all components, yarns and matrix are considered at failure.
2. Undulated yarns are considered at complete failure only if 90% of subdivisions-UD composites are damaged.
3. A multi-failure mode is assigned to the failed subdivisions-UD composites.
4. The applied stress on the REV increases only if no new failure is observed.

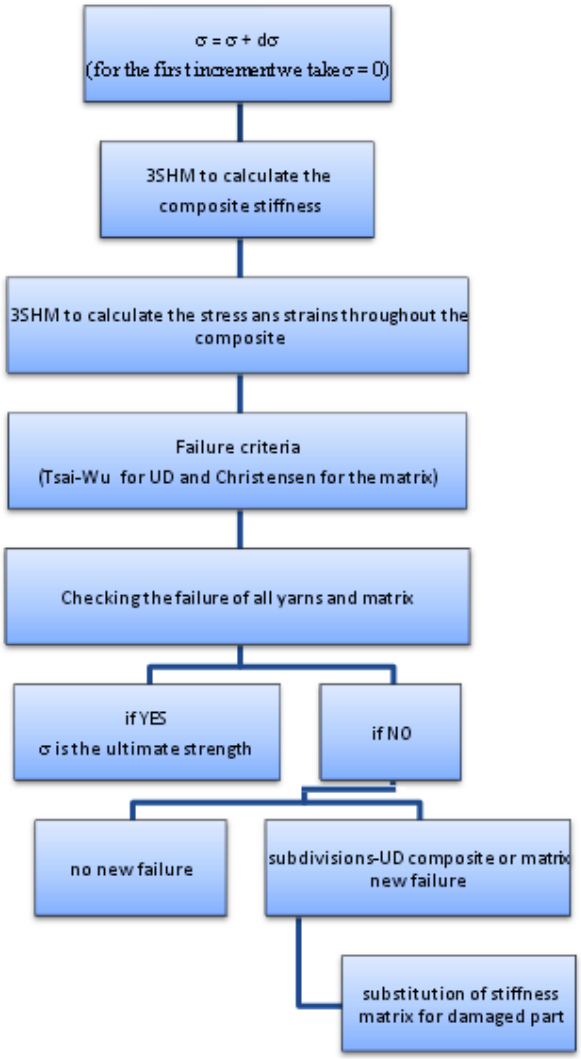

Figure 1. General Scheme of the evaluation of the ultimate strength under static loading of textile composites Geometrical modeling

Defining the Representative Elementary Volume (REV) is the first step in the geometrical modeling for any analytical model as shown in Figure 2. The geometrical parameters, such as the length, width and height of the REV, also the height and width of each yarn cross-sectional area should be determined.

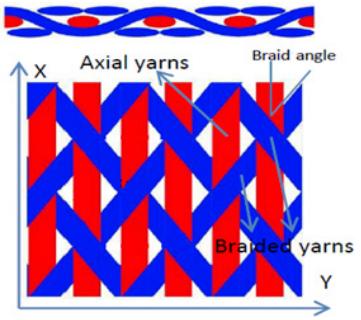

Figure 2. REV for a 2D tri-axially braided composite

For undulated braided yarns, it can be modeled by a sinusoidal shape. An undulated yarn in the (XZ) plane is taken as example as shown in Figure 3. The undulated part of yarn is modeled by its centerline with a sinusoidal function:

$$Z(x) = a.\cos(2\pi x/T) \quad (1)$$

With:

Left undulated section: $T/2 \leq x \leq T$;

Right undulated section: $0 \leq x \leq T/2$;

Where "a" and "T" are the amplitude and the period, respectively. They are calculated in terms of geometrical parameters according to the composite architecture.

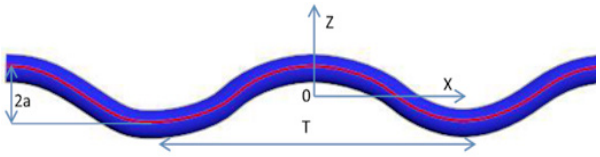

Figure 3. Sinusoidal shape of an undulated yarn

The volume of the entire undulated part:

$$V_{und} = A \cdot L_{und} \quad (2)$$

Where A is the area of transversal section and L_{und} is the length of the centreline of the undulated part given by:

$$L_{und} = \begin{cases} \int_0^{T/2} \sqrt{1+\left(\frac{d_z}{d_x}\right)^2}\, d_x & at\ right \\ \int_{-T/2}^{0} \sqrt{1+\left(\frac{d_z}{d_x}\right)^2}\, d_x & at\ left \end{cases} \quad (3)$$

Where:

$$\left(\frac{d_z}{d_x}\right)^2 = \left(a \cdot \frac{2\pi}{T} \cdot \sin\left(\frac{2\pi x}{T}\right)\right)^2 \quad (4)$$

The calculation of fiber volume fractions in the composite Vf_c and in each yarn Vf_y is very important in determining the stiffness matrix of the composite. Thus, there are many analytical methods where Vf_y could be determined, depends on available experimental data of the studied composite.

Knowing that almost all experimental data of composites give the value of Vf_c. However, Vf_y can be calculated in terms of REV and yarns volumes:

$$Vf_y = \frac{Vf_c \cdot V_{REV}}{V_{Yarns}} \quad (5)$$

In this method, it's assumed that all yarns have the same fiber volume fraction.

2.1. Analytical Homogenization Method (3SHM model)

In this section, the homogenization method required to determine the elastic properties and composite stiffness matrix is briefly presented. Moreover, this method is used to predict the stress and strain fields throughout the REV "Representative Elementary Volume". The homogenization method was developed earlier in order to predict the elastic properties of textile composites.

Geometrical modeling is employed for the discretization of undulated yarns and the calculation of fibers orientations and sizes of sub-volumes. Concerning the homogenization method, the 3SHM model presents three stages of homogenization levels: micro, meso and macro homogenization stages. At the first stage, the stiffness matrices of sub-volumes are calculated. Then, at the meso homogenization stage the stiffness matrices of yarns are evaluated by assembling sub-volumes using a combined iso-strain and iso-stress method. Finally, at the macro stage, the stiffness of the REV is evaluated in terms of the homogenized yarns and the matrix stiffness matrices under an iso-strain assumption as shown in Figure 4.

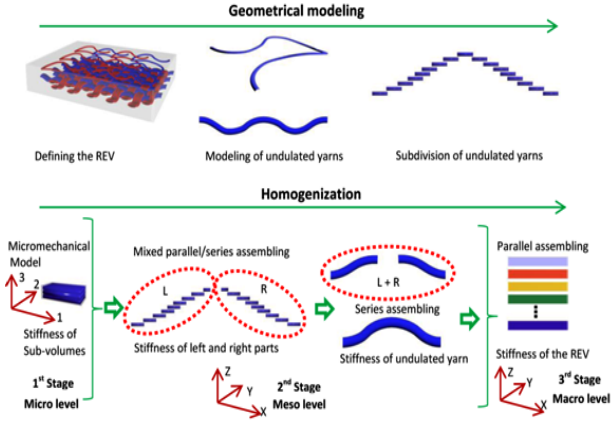

Figure 4. The homogenization scheme of the 3SHM model

At the micro level homogenization, the discretized small sub-volumes of undulated yarn, in addition to the straight yarns, are considered as unidirectional lamina with long fibers. They represent transversely isotropic materials. Their effective elastic properties are found using a micromechanical analytical model as described in the previous section. Then, stiffness matrices of yarns sub-volumes $\left[C_{ui}^{123}\right]$ are known in the local coordinate system (123) in terms of compliance matrix

$$\left[C_{ui}^{123}\right] = \left[S_{ui}^{123}\right]^{-1} \quad (6)$$

$$\left[S_{ui}^{123}\right] = \begin{bmatrix} \frac{1}{E_{11}} & \frac{-V_{12}}{E_{11}} & \frac{-V_{12}}{E_{11}} & 0 & 0 & 0 \\ \frac{-V_{12}}{E_{11}} & \frac{1}{E_{22}} & \frac{-V_{23}}{E_{22}} & 0 & 0 & 0 \\ \frac{-V_{12}}{E_{11}} & \frac{-V_{23}}{E_{22}} & \frac{1}{E_{22}} & 0 & 0 & 0 \\ 0 & 0 & 0 & \frac{1}{G_{23}} & 0 & 0 \\ 0 & 0 & 0 & 0 & \frac{1}{G_{12}} & 0 \\ 0 & 0 & 0 & 0 & 0 & \frac{1}{G_{12}} \end{bmatrix} \quad (7)$$

$\left[S_{ui}^{123}\right]$ is the compliance matrix of a transversely isotropic material.

There are many analytical micromechanical models used to predict the elastic properties of unidirectional lamina with long fibers. Some micromechanical models are also used to evaluate the ultimate strength of UD composites. Based on a comparative study done previously [15], the Chamis micromechanical model [13, 14] is used to evaluate the elastic properties and ultimate strength for a UD composite.

The matrix is considered to be an isotropic material where the stiffness matrix $[C_m]$ can be simply derived from the compliance matrix $[S_m]$ in terms of Young's modulus E_m and the Poisson's ratio ν_m.

$$[S_m]=\begin{bmatrix} \frac{1}{E_m} & \frac{-\nu_m}{E_m} & \frac{-\nu_m}{E_m} & 0 & 0 & 0 \\ \frac{-\nu_m}{E_m} & \frac{1}{E_m} & \frac{-\nu_m}{E_m} & 0 & 0 & 0 \\ \frac{-\nu_m}{E_m} & \frac{-\nu_m}{E_m} & \frac{1}{E_m} & 0 & 0 & 0 \\ 0 & 0 & 0 & \frac{E_m}{2\cdot(1+\nu_m)} & 0 & 0 \\ 0 & 0 & 0 & 0 & \frac{E_m}{2\cdot(1+\nu_m)} & 0 \\ 0 & 0 & 0 & 0 & 0 & \frac{E_m}{2\cdot(1+\nu_m)} \end{bmatrix} \quad (8)$$

At the meso level homogenization, the stiffness matrices of the undulated yarns are evaluated. The stiffness of an undulated yarn is evaluated using both iso-strain and iso-stress assumptions when assembling sub-volumes respecting the following scheme:

1- The stiffness and compliance matrices of sub-volumes in the (XYZ) coordinate system are given by:

$$C_{ui}^{xyz}=T_c\cdot C_{ui}^{123}\cdot T_c^t \quad (9)$$

$$S_{ui}^{xyz}=T_s\cdot S_{ui}^{123}\cdot T_s^t \quad (10)$$

Where T_c and T_s are the 3D transformation matrices.

2- The sub-volumes of left and right undulated parts (referred by L and R respectively) as shown in Figure 5 are assembled in a mixed iso-strain /iso-stress model using a weighted parameter P_{cu}, where the stiffness matrices of left and right undulated parts are given respectively by:

$$\left[C_{lu}^{xyz}\right]=P_{cu}\frac{\sum_{i=1}^{n}V_{Lui}\cdot C_{Lui}^{xyz}}{V_{Lu}}+(1-P_{cu})\cdot\left[\frac{\sum_{i=1}^{n}V_{Lui}\cdot S_{Lui}^{xyz}}{V_{Lu}}\right]^{-1} \quad (11)$$

$$\left[C_{Ru}^{xyz}\right]=P_{cu}\frac{\sum_{i=1}^{n}V_{Rui}\cdot C_{Rui}^{xyz}}{V_{Ru}}+(1-P_{cu})\cdot\left[\frac{\sum_{i=1}^{n}V_{Rui}\cdot S_{Rui}^{xyz}}{V_{Ru}}\right]^{-1} \quad (12)$$

$$P_{cu}=2\cdot\frac{\overline{\theta}}{\pi} \quad (13)$$

V_{Lui} : Volume of the ith sub-volume of the left undulated part

V_{Rui} : Volume of the ith sub-volume of the right undulated part

V_{Lu} : Volume of the left undulated part

V_{Ru} : Volume of the right undulated part

$\overline{\theta}$: The mean value of the inclination angle of sub-volumes "$\overline{\theta}$" of a subdivided undulated yarn.

Noting that in general and due to the symmetry of left and right undulated parts, we have:

$$V_{Lu}=V_{Ru}$$

P_{cu} has the same value for both parts. The yarn is composed of homogenized left and right undulated parts which form a series system when assembled along undulation direction as shown in Figure 5.

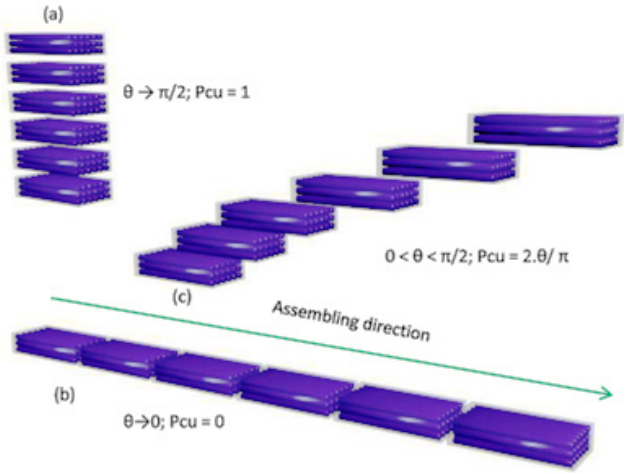

Figure 5. (a) Parallel system, (b) series system, (c) sub-volumes of actual undulated yarn

The iso-stress model is then used to evaluate the stiffness of the undulated yarn (left + right):

$$\left[S_u^{xyz}=\frac{V_{Lu}\cdot\left[C_{Lu}^{xyz}\right]^{-1}+V_{Ru}\cdot\left[C_{Rc}^{xyz}\right]^{-1}}{V_u}\right] \quad (14)$$

$$\left[C_U^{xyz}\right]=\left[S_U^{xyz}\right]^{-1} \quad (15)$$

Where V_n is the volume of the yarn.

At the macro level homogenization stage, the stiffness of the REV is evaluated in terms of the previously evaluated stiffness matrices of the matrix and the n yarns. Therefore, the composite is treated as n+1 homogenized block assumed to represent a parallel system and assembled under an iso-strain condition:

$$C_{REV}=\frac{\sum_{K=1}^{k=n}V_U^K\cdot C_U^K+V_m\cdot C_m}{V_{REV}} \quad (16)$$

Where V_m and V_{REV} are the volumes of the matrix and the REV, respectively.

2.2. Evaluation of the Stress-strain Fields throughout the Composite

In order to apply the failure criterion and the damaged stiffness model, the stress and strain fields for each subdivision-UD composite should be calculated. This could be done using the 3SHM model. An inverse procedure of that used to determine the elastic properties is applied. Let us consider a textile composite which consists of n yarns and a polymeric matrix. The generalized homogenization method (3SHM), allows the calculation of stress and strain fields throughout the composite as follows:

The average stress tensor throughout the composite is given by:

$$\left\{\overline{\sigma_c}\right\}=\frac{1}{V_c}\iiint\left\{\sigma_c\right\}\cdot d_V \tag{17}$$

The Hook's law gives:

$$\left\{\overline{\sigma_c}\right\}=\left[C_c\right]\cdot\left\{\overline{\varepsilon_c}\right\} \tag{18}$$

Where $\left[C_c\right]$ is the stiffness matrix of the composite

The iso-strain conditions gives:

$$\left\{\overline{\varepsilon_c}\right\}=\left\{\overline{\varepsilon_{y1}}\right\}=\left\{\overline{\varepsilon_{y2}}\right\}=\ldots=\left\{\overline{\varepsilon_{yn}}\right\}=\left\{\overline{\varepsilon_m}\right\} \tag{19}$$

Where: $\left\{\overline{\varepsilon_c}\right\}$, $\left\{\overline{\varepsilon_{y1}}\right\}$, $\left\{\overline{\varepsilon_{y2}}\right\}$, $\left\{\overline{\varepsilon_{yn}}\right\}$ and $\left\{\overline{\varepsilon_m}\right\}$ are the average strain in the composite and the n yarns and matrix

The stress throughout the matrix is given by:

$$\left\{\overline{\sigma_m}\right\}=\left[C_m\right]\cdot\left\{\overline{\varepsilon_m}\right\} \tag{20}$$

Where $\left[C_m\right]$ is the stiffness matrix of the matrix

The stress throughout the n yarns is given by:

$$\left\{\overline{\sigma_{yi}}\right\}=\left[C_{yi}\right]\cdot\left\{\overline{\varepsilon_{y1}}\right\} \tag{21}$$

Where $\left[C_{yi}\right]$ is the stiffness matrix of the ith yarn

Then, the stress throughout each subdivision of each yarn should be calculated as follow:

An iso-stress condition is considered for the left and right parts of the undulated yarns:

$$\left\{\overline{\sigma_{right\ \ part\ yi}}\right\}=\left\{\overline{\sigma_{left\ \ part\ yi}}\right\}=\left\{\overline{\sigma_{yi}}\right\} \tag{22}$$

Then, to calculate the stress throughout each subdivision, a mixed iso-stress and iso-strain conditions are considered. The iso-strain condition means that the strain in the undulated yarns equal to that for each subdivision:

$$\left\{\overline{\varepsilon_{y1}}\right\}=\left[S_{yi}\right]\cdot\left\{\overline{\sigma_{yi}}\right\} \tag{23}$$

Where $\left[S_{yi}\right]$ is the compliance matrix of the ith yarn

$$\left\{\overline{\varepsilon_{y1}}\right\}=\left\{\overline{\varepsilon_1}\right\}=\left\{\overline{\varepsilon_2}\right\}=\cdots=\left\{\overline{\varepsilon_{yn}}\right\} \tag{24}$$

Where $\left\{\overline{\varepsilon_{y1}}\right\}$, $\left\{\overline{\varepsilon_1}\right\}$, $\left\{\overline{\varepsilon_2}\right\}$, … and $\left\{\overline{\varepsilon_n}\right\}$ are the average strains in the undulated right/left part of the ith yarn.

$$\left\{\overline{\sigma'_i}\right\}=\left[C_i\right]\cdot\left\{\overline{\varepsilon_1}\right\} \tag{25}$$

Where $\left\{\overline{\sigma'_i}\right\}$, $\left\{\overline{\varepsilon_1}\right\}$ and $\left[C_{yi}\right]$ are the stress, strain and the stiffness matrix respectively of the ith yarn under iso-stress condition

$$\left\{\overline{\sigma_{y1}}\right\}=\left\{\overline{\sigma''_1}\right\}=\left\{\overline{\sigma''_2}\right\}=\cdots=\left\{\overline{\sigma''_{yn}}\right\} \tag{26}$$

The stress throughout the subdivision in the (xyz) global coordinate system is given by:

$$\left\{\overline{\sigma_i}\right\}=\text{Pc}.\left\{\overline{\sigma'_i}\right\}+(1\text{-Pc}).\left\{\overline{\sigma''_i}\right\} \tag{27}$$

Finally, the stress in local coordinate system is calculated using a transformation matrix as follows:

$$\left\{\overline{\sigma_i}\right\}^{xyz}=T_c\cdot\left\{\overline{\sigma_i}\right\}^{123} \tag{28}$$

2.3. Failure Criteria for Subdivision-UD Composite and Matrix

The failure criterion proposed to predict the failure of UD composites is a tensor polynomial criterion proposed by Tsai and Wu [12]. This criterion is used for subdivision-UD composite and straight yarns. This criterion may be expressed in tensor notation as:

$$F_i\sigma_i+F_{ij}\sigma_i\sigma_j+F_{ijk}\sigma_i\sigma_j\sigma_k\geq 1 \tag{29}$$

where i, j, k = 1, ... , 6 for a 3D case. The parameters F_i, F_{ij} and F_{ijk} are related to the lamina strengths in the principal directions. For practical purposes, and due to the large number of material constants required, the third-order tensor Fijk is usually neglected. Therefore, the general polynomial criterion reduces to a general quadratic expression given by:

$$F_i\sigma_i+F_{ij}\sigma_i\sigma_j\geq 1 \tag{30}$$

where i, j = 1, ... , 6. Considering that the failure of the material is insensitive to a change of sign in shear stresses, all terms containing a shear stress to first power must vanish: F4 = F5 =F6 = 0. Then, the explicit form of the general expression is:

$$F_1\sigma_1+F_2\sigma_2+F_3\sigma_3+2F_{12}\sigma_1\sigma_2+2F_{13}\sigma_1\sigma_3+2F_{23}\sigma_2\sigma_3$$
$$+F_{11}\sigma_1^2+F_{22}\sigma_2^2+F_{33}\sigma_3^2+F_{44}\sigma_4^2+F_{55}\sigma_5^2+F_{66}\sigma_6^2\geq 1 \tag{31}$$

Where

$$F_1=\frac{1}{X_t}-\frac{1}{X_c};\ F_1=\frac{1}{X_t}-\frac{1}{X_c};\ F_1=\frac{1}{X_t}-\frac{1}{X_c}$$

$$F_{11}=\frac{1}{X_t\cdot X_c};\ F_{22}=\frac{1}{Y_t\cdot Y_c};\ F_{33}=\frac{1}{Z_t\cdot Z_c}$$

$$F_{44}=\frac{1}{Q^2};\ F_{55}=\frac{1}{R^2};\ F_{66}=\frac{1}{S^2}$$

Where

Xt, Xc, Yt, Yc, Zt and Zc are the ultimate axial strengths for UD composites calculated by Chamis model [13, 14], where t is for tensile and c for compression in x, y and z directions. Also, Q, R and S are the ultimate shear strengths

for UD composites, where Q and R are for out of plane shear and S is for in-plane shear.

Concerning the failure of the pure matrix, the Christensen's failure criterion is adopted as follows:

$$\left(\frac{1}{X_{tm}}-\frac{1}{X_{cm}}\right)\cdot(\sigma_1+\sigma_2+\sigma_3)+\frac{1}{X_{tm}X_{cm}}\left\{\frac{1}{2}\cdot\left[(\sigma_1-\sigma_2)^2+(\sigma_2-\sigma_3)^2+(\sigma_3-\sigma_1)^2\right]+3\cdot(\sigma_{12}^2+\sigma_{13}^2+\sigma_{23}^2)\right\}\le 1 \quad (32)$$

Where σ_I is the maximum tensile stress at a point which is the maximum value of the three roots of the following cubic equation:

$$\sigma_1^3-(\sigma_1+\sigma_2+\sigma_3)\cdot\sigma_1^2+(\sigma_1\sigma_2+\sigma_2\sigma_3+\sigma_1\sigma_3-\sigma_{12}^2-\sigma_{23}^2-\sigma_{13}^2)\cdot\sigma_1-(\sigma_1\sigma_2\sigma_3-\sigma_1\sigma_{23}^2-\sigma_2\sigma_{13}^2-\sigma_3\sigma_{12}^2+2\sigma_{12}\sigma_{23}\sigma_{13})=0 \quad (33)$$

2.4. Damaged Stiffness Model for UD Composites and Matrix

The damaged stiffness model tends to replace the stiffness of UD composites or the matrix at failure by a reduced stiffness matrix. The complete failure of a subdivision-UD composite could happen under different failure modes. As discussed, in recent works, the method used is based on determining the major loading that causes the failure, and then assigning a corresponding failure mode in order to replace the stiffness of UD composites by a specific damaged stiffness matrix related to that failure mode.

However, assigning one failure mode for each damaged subdivision-UD composite could lead to huge errors due to the modeling of textile composites with complex undulated yarns. In order to overcome this problem the influence of all stresses acting on a UD composite is taken into account. Different failure modes should be considered. The failure modes, as given by [18], consist of: Tensile and compressive axial failure modes along x, y and z direction, and shear failure modes for both positive and negative applied shear stress. The failure modes are shown in Figure 6:

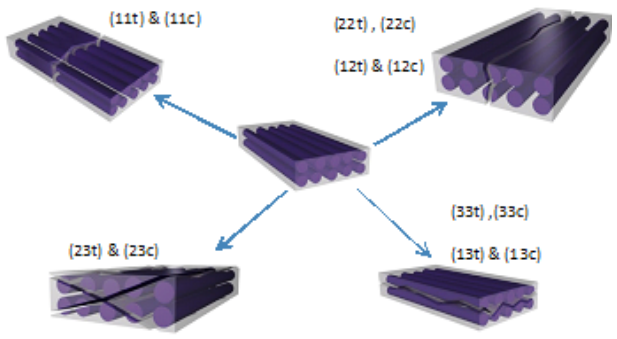

Figure 5. Failure modes

Axial tensile stress failure mode (11t) and axial compressive stress failure mode (11c); Transversal tensile stress failure mode (22t) and transversal compressive stress failure mode (22c); Transversal out of plane tensile stress failure mode (33t) and transversal out of plane compressive stress failure mode (33c); Positive in-plane shear stress failure mode (12t) and negative in-plane shear stress failure mode (12c); Positive in-plane shear stress failure mode (13t) and negative in-plane shear stress failure mode (13c); Positive in-plane shear stress failure mode (23t) and negative in-plane shear stress failure mode (23c).

The damaged stiffness is considered as combination of different damage stiffness matrices corresponding to different failure modes. The damaged stiffness is written as follows:

C_{UD} damage = R11t.C11t + R11c.C11c + R22t.C22t + R22c.C22c + R33t.C33t + R33c.C33c + R23t.C23t + R23c.C23c + R13t.C13t + R13c.C13c + R12t.C12t + R12c.C12c.

The coefficients "R" are the ratios of the applied stress over the corresponding ultimate strength. Matrices "C" are the damaged stiffness matrices corresponding to a specific failure mode. For a damaged subdivision, the elastic properties are recalculated in terms of those given by the Chamis model [13, 14], according to the failure mode. Then, the corresponding damaged stiffness matrices are composed using the above reduced elastic properties.

The matrix is considered polymeric for an isotropic material. A damaged stiffness matrix is used when the matrix is at failure. The damaged stiffness matrix is recalculated in terms of reduced elastic properties as follows [18]:

$$E_m=0.01E_m \quad \text{and} \quad G_m=0.2G_m$$

2.5. Damaged Stiffness Model

Hereafter the following ratios and the reduced elastic properties

$R_{11t}=\frac{\sigma_x}{X_t}$ (ratio of stresses along x direction)

$R_{11c}=\frac{\sigma_x}{X_c}$ (ratio of stresses along x direction)

$R_{22t}=\frac{\sigma_y}{Y_t}$ (ratio of stresses along y direction)

$R_{22c}=\frac{\sigma_y}{Y_c}$ (ratio of stresses along y direction)

$R_{33t}=\frac{\sigma_z}{Y_t}$ (ratio of stresses along z direction)

$R_{33c}=\frac{\sigma_z}{Y_c}$ (ratio of stresses along z direction)

$R_{12t}=\frac{\tau_{xy}}{\tau_{xyu}}$ (ratio of in-plane (xy) shear stresses for positive applied shear); $R_{12c}=\frac{\tau_{xy}}{\tau_{xyu}}$ (ratio of in-plane (xy) shear stresses for negative applied shear)

$R_{13t} = \frac{\tau_{xz}}{\tau_{xzu}}$ (ratio of in-plane (xz) shear stresses for positive applied shear); $R_{13c} = \frac{\tau_{xz}}{\tau_{xzu}}$ (ratio of in-plane (xz) shear stresses for negative applied shear)

$R_{23t} = \frac{\tau_{yz}}{\tau_{yzu}}$ (ratio of in-plane (yz) shear stresses for positive applied shear); $R_{23c} = \frac{\tau_{yz}}{\tau_{yzu}}$ (ratio of in-plane (yz) shear stresses for negative applied shear)

Axial tensile stress failure mode (11t): $E_{11} = 0.01E_{11}$, $G_{12} = 0.01G_{12}$, $G_{13} = 0.01G_{13}$ and $v_{12} = 0.01v_{12}$.

Axial compressive stress failure mode (11c): $G_{12} = 0.01G_{12}$, $G_{13} = 0.01G_{13}$.

Transversal tensile stress failure mode (22t): $E_{22} = 0.01E_{22}$, $G_{12} = 0.01G_{12}$, $G_{23} = 0.01G_{23}$ and $v_{23} = 0.01v_{23}$.

Transversal compressive stress failure mode (22c): $G_{12} = 0.01G_{12}$, $G_{23} = 0.01G_{23}$.

Transversal out of plane tensile stress failure mode (33t): $E_{33} = 0.01E_{33}$, $G_{13} = 0.01G_{13}$, $G_{23} = 0.01G_{23}$ and $v_{13} = 0.01v_{13}$.

Transversal out of plane compressive stress failure mode (33c): $G_{13} = 0.01G_{13}$, $G_{23} = 0.01G_{23}$

Positive in-plane shear stress failure mode (12t): same as failure mode (22t).

Negative in-plane shear stress failure mode (12c): same as failure mode (22c).

Positive in-plane shear stress failure mode (13t): same as failure mode (33t).

Negative in-plane shear stress failure mode (13c): same as failure mode (33c).

Positive in-plane shear stress failure mode (23t): $E_{22} = 0.01E_{22}$, $G_{12} = 0.01G_{12}$, $G_{13} = 0.01G_{13}$, $G_{23} = 0.01G_{23}$ and $v_{23} = 0.01v_{23}$.

Negative in-plane shear stress failure mode (23c): $E_{22} = 0.01E_{22}$, $G_{12} = 0.01G_{12}$, $G_{13} = 0.01G_{13}$, $G_{23} = 0.01G_{23}$ and $v_{23} = 0.01v_{23}$.

3. Results and Discussion

First of all, the model is validated through a modeling of tri-axially braided composite [19] found in literature. A good agreement is found between the elastic properties and ultimate strengths where the error is less than 10% as shown in Tables 1 and 2. The elastic moduli are in GPa and the strengths are in MPa.

Table 1. Elastic properties for different braided composites predicted by the proposed model compared to available experimental data [19]

Type	Method	E_x	E_y	E_z	G_{xy}	G_{xz}	G_{yz}
Br-30	Analy	71.4	12.6	9.8	15.9	5.7	3.9
	Exp	68.9			14.9		
	Diff %	4			7		
Br-45a	Analy	47.5	22.5	9.4	23.3	4.2	3.8
	Exp	44.1	21.4		25.0		
	Diff %	8	5		-7		
Br-45b	Analy	47.2	21.6	9.4	21.3	4.2	3.8
	Exp	46.4					
	Diff %	2					

Table 2. Ultimate strengths for different braided composites predicted by the proposed model compared to available experimental data [19]

Type	Method	σ_x	σ_y	σ_z	τ_{xy}	τ_{xz}	τ_{yz}
Br-30	Analy	635	90	90	90	60	60
	Exp	710					
	Diff %	11					
Br-45a	Analy	510	170	90	180	60	60
	Exp	451	178				
	Diff %	13	-4				
Br-45b	Analy	515	160	90	165	60	60
	Exp	458					
	Diff %	12					

After validation of the model, a parametric study is now presented. Table 3 shows the mechanical properties that will be used in this study.

Table 3. Mechanical properties of various kinds of fibers and epoxy

Material property	AS4 -carbon fiber	S2-glass	Epoxy
Axial modulus E_{f1}	231	87	3.2
Transverse modulus E_{f2}	15	87	3.2
In-plane shear modulus G_{f12}	15	36	1.2
Transverse shear modulus G_{f23}	7	36	1.2
Major Poisson's ratio v_{12}	0.2	0.2	0.35
Major Poisson's ratio v_{23}	0.2	0.2	0.35
Axial tensile strength X_{f1T}	3500	2850	85
Axial compressive strength X_{f1C}	3000	2450	120
Shear strength S_m	_	_	50

Figure 7 shows that the axial Young's modulus E_x decreases with the increment of the braid angle. The transversal Young's modulus E_y increases with the increment of the braid angle. This is due to the increment of the rigidity in the y-direction and its decrement in the x-direction. In addition, the transversal and axial Young's moduli intersect at the braid angle θ=56° for all fraction volumes, which means that the composite will behave as an isotropic material, knowing that the AS4 carbon fiber is an anisotropic material.

Figure 8 shows that, the S2 glass "an isotropic material" have the same behavior as AS4. The transversal and axial Young's moduli intersect at the braid angle θ=56° for all fraction volumes. Therefore, we can conclude that the behavior of a 2D tri-axially braided composite is independent of the type of material for the in-plane Young's moduli, and depends only on the geometry. For any type of fibers, the behavior of in-plane Young's moduli for the composite will be the same.

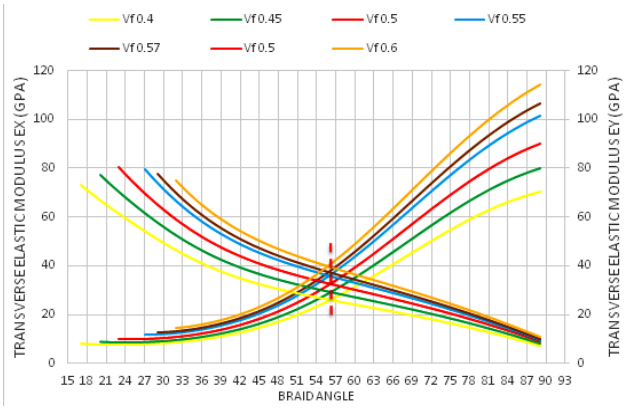

Figure 6. Effect of the braid angle on in-plane Young's modulus (E_x and E_y) for different fraction volume V_f for the AS4 carbon fiber

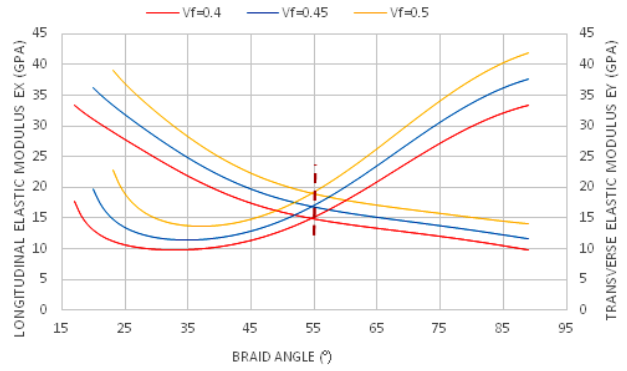

Figure 7. Effect of the braid angle on in-plane Young's modulus (E_x and E_y) for different fraction volume V_f for the S2-glass fiber

Figure 9 shows that, the in-plane shear modulus G_{xy}, increases with the increment of the braid angle and reaches its peak at θ=47°, in all fraction volumes. This is due to the braided yarns that reinforce the in-plane shear modulus by preventing sliding between yarns. In addition, it is observed that between the angles 40° and 50°, the highest range of G_{xy} is obtained. For the S2 glass as shown below in Figure 10, the in-plane shear modulus G_{xy}, increases with the increment of the braid angle and reaches its peak at θ=47^0, in all fraction volumes.

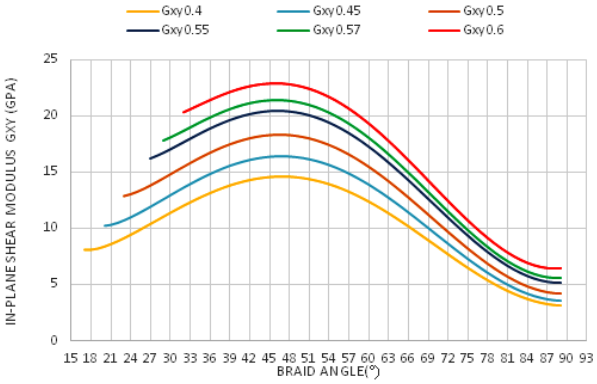

Figure 8. Effect of the braid angle on in-plane shear modulus G_{xy} for different fraction volume V_f for the AS4 carbon fiber

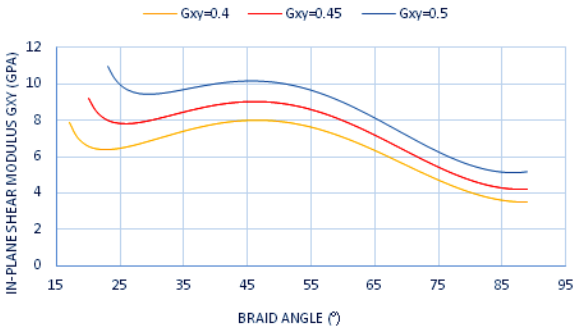

Figure 9. The effect of braid angle on in-plane shear modulus G_{xy} for different fraction volume V_f for the S2-galss

The in-plane Poisson's ratio v_{xy}, is higher than the other Poisson's ratios at $\theta \leq 45°$, as shown in Figure 11. Where, the reinforcement of the braided yarns in the axial direction is larger than in the y-direction at $\theta \leq 45°$. This means, that the dilatation in the lateral direction in this range is higher than the axial direction, which is relatively small. Moreover, the other Poisson's ratios v_{xz} and v_{yz} are nonlinearly varying with the increment of the braid angle.

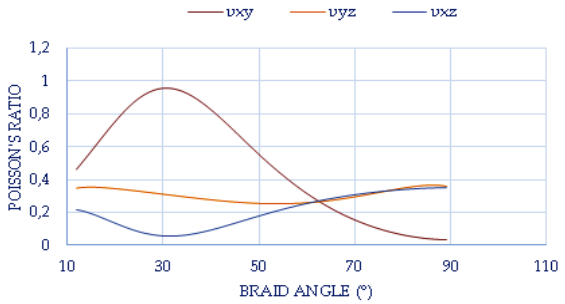

Figure 10. Effect of the braid angle on Poisson's ratio (v) for fraction volume V_f =0.35 for the AS4 carbon fiber

Figure 12 shows that there is no significant change in the Poisson's ratio as the fraction volume V_f increases from 0.3 to 0.6 in AS4 carbon fiber. This means that the Poisson's ratio depends on the braid angle only. To improve this conclusion, Figure 12 also shows the in-plane Poisson's ratio for S2-glass which is an isotropic material and has the same behavior for the same range of angles. There is no significant change in the Poisson's ratio as the fraction volume V_f increases from 0.4 to 0.5, but there is a difference in the maximum values of the Poisson's ratio between AS4 carbon fiber and S2-glass which must effectively depends on the material properties.

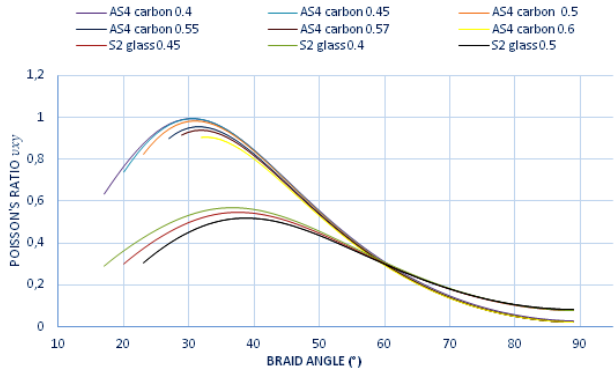

Figure 11. Effect of the braid angle on the in-plane Poisson's ratio (v_{xy}) for different fraction volume V_f for both AS4 carbon fiber and S2-glass

Figure 13 shows the axial strength S_x, which decreases with the increment of the braid angle, while the transversal strength S_y increases with the increment of the braid angle. This is due to the increment of the rigidity in the y-direction as a result of the increment of the braid angle. In addition, the transversal and axial strengths intersect between the braid angle θ=62^0 and θ=67^0 as the fraction volumes change from 0.35 to 0.6.

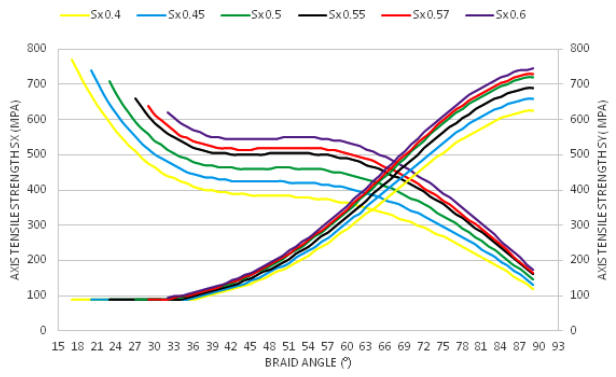

Figure 12. Effect of the braid angle on in-plane tensile strength (S_x and S_y) for different fraction volume V_f for the AS4 carbon fiber

Figure 14 shows the axial strength S_x, which decreases with the increment of the braid angle, while the transversal strength S_y increases with the increment of the braid angle. In addition, the strengths of S2 glass do not intersect between the transversal and axial strengths, due to the isotropic behavior of the fibers. Therefore, as a conclusion, the effect is dual, depending on the fibers' material and the geometry. However, in the modulus of elasticity, it was the effect of geometry only.

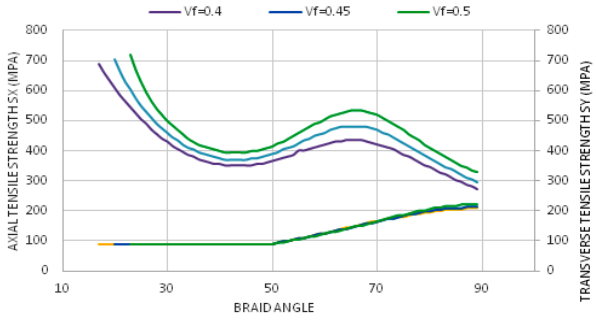

Figure 13. Effect of the braid angle on in-plane tensile strength (S_x and S_y) for different fraction volume V_f for the S2-glass

Figure 15 shows the in-plane shear strength S_{xy} for AS4 carbon fiber, which increases with the increment of braid angle, and reaches its peak between θ= 45^0 and θ= 52^0 in all fraction volumes. This is due to the braided yarns that reinforce the in-plane shear strength by preventing sliding between yarns.

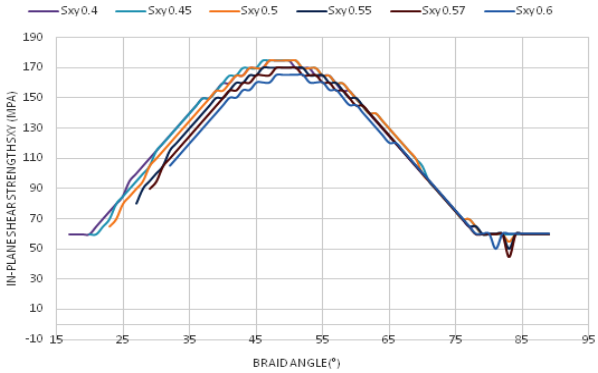

Figure 14. Effect of the braid angle on in-plane shear strength S_{xy} for different fraction volume V_f for the As4 carbon fiber

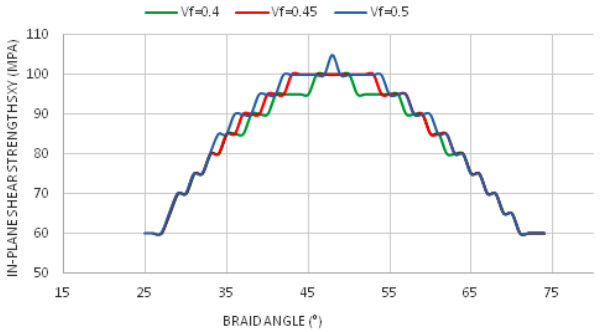

Figure 15. Effect of the braid angle on in-plane shears strength S_{xy} for different fraction volume V_f for the S2-glass

In Figure 16, the shear strength's behaviors for S2 glass are the same as of the AS4 carbon fiber behavior. The behavior of in-plane shear strength S_{xy} is independent of the material of the fibers and the effect is related to the geometry where the maximum still between the angles $\theta = 45^0$ and $\theta =$ 52° in all cases.

4. Conclusions

The proposed model consists of four main parts: a micromechanical modeling for elastic properties and ultimate strengths for unidirectional composites (UD composites), a homogenization method at meso and macro levels to determine the composite stiffness and stress-strain fields throughout the composite, two 3D failure criteria for the matrix and UD composites and a damaged stiffness model. At first, a modeling of some tri-axially braided composites is performed where the predicted elastic properties and ultimate strengths are compared to available experimental data and numerical Finite element predictions. After validating the reliability of the analytical model, a parametric study is done.

The obtained results are analyzed in order to investigate the influence of each parameter (Fiber type, V_f and braid angle) on the mechanical properties of braided composites. Some significant remarks are found; at specific angle for different type of fibers and different values of V_f the in-plane Young's moduli are similar. In addition, at a closer angle the highest values of in-plane shear modulus and shear strengths are found. The analysis shows clearly how the influence of the braid angle could be significant. It also shows that for some high value of V_f the improvement in mechanical properties especially ultimate strengths is not so important.

As a conclusion, this work proposed a parametric study based on analytical modeling which leads to a better choice of braided fabric architecture to achieve the optimum design of a composite structure. Also, it shows that the same study could be done for any kind of fiber reinforcement and polymeric matrix providing a data sheet for engineers and designers.

REFERENCES

[1] Byun, J. H., Whitney, T. J., Du, G. W., & Chou, T. W. (1991). Analytical characterization of two-step braided composites. *Journal of composite materials*, *25*(12), 1599-1618.

[2] Shokrieh, M. M., & Mazloomi, M. S. (2010). An analytical method for calculating stiffness of two-dimensional tri-axial braided composites. *Composite Structures*, *92*(12), 2901-2905.

[3] Quek, S. C., Waas, A. M., Shahwan, K. W., & Agaram, V. (2003). Analysis of 2D triaxial flat braided textile composites. *International Journal of Mechanical Sciences*, *45*(6), 1077-1096.

[4] Tsai, K. H., Hwan, C. L., Chen, W. L., & Chiu, C. H. (2008). A parallelogram spring model for predicting the effective elastic properties of 2D braided composites. *Composite Structures*, *83*(3), 273-283.

[5] Xiao, X., Kai, H.G., Gong X., (2011). Strength predictions of a triaxially braided composite. *Composites Part A: Applied Science and Manufacturing, 42*, 1000–1006.

[6] Yan, Y., Hoa, S.V., (2002). Energy model for prediction of mechanical behavior of 2-D triaxially braided composites, Part II: parameter analysis. *Journal of composite materials*, *36*, 1233-1253.

[7] Zhang, C., Binienda, K.W., Kohlman, L.W., (2014). Analytical model and numerical analysis of the elastic behavior of triaxial braided composites. *Journal of Aerospace Engineering, 27*, 473–483.

[8] Zhang, P., Gui, L.J., Fan, Z.J., (2009). An analytical model for predicting the elastic properties of triaxially braided composites. *Journal of Reinforced Plastics and Composites, 28*, 1903–1916.

[9] Li, D. S., Lu, Z. X., Chen, L., & Li, J. L. (2009). Microstructure and mechanical properties of three-dimensional five-directional braided composites. *International journal of solids and structures*, *46*(18), 3422-3432.

[10] Jiang, L., Zeng, T., Yan, S., & Fang, D. (2013). Theoretical prediction on the mechanical properties of 3D braided composites using a helix geometry model. *Composite Structures*, *100*, 511-516.

[11] Hallal, A., Younes, R., & Fardoun, F. (2013). Review and comparative study of analytical modeling for the elastic properties of textile composites. *Composites Part B: Engineering*, *50*, 22-31.

[12] Hallal, A., Younes, R., Fardoun, F., & Nehme, S. (2012). Improved analytical model to predict the effective elastic properties of 2.5 D interlock woven fabrics composite. *Composite Structures*, *94*(10), 3009-3028.

[13] Chamis, C. C. (1989). Mechanics of composite materials: past, present and future. *Journal of composites technology & research*, *11*(1), 3-14.

[14] Chamis, C. C., Abdi, F., Garg, M., Minnetyan, L., Baid, H., Huang, D. & Talagani, F. (2013). Micromechanics-based progressive failure analysis prediction for WWFE-III composite coupon test cases. *Journal of Composite Materials*, *47 (*20–21), 2695–2712.

[15] Hallal, A., Fardoun, F., Younes, R., & Hage Chehade, F. (2011, October). Evaluation of longitudinal and transversal Young's moduli for unidirectional composite material with long fibers. In *Advanced Materials Research* (Vol. 324, pp. 189-192).

[16] Tsai, S. W., & Wu, E. M. (1971). A general theory of strength for anisotropic materials. *Journal of composite materials*, *5*(1), 58-80.

[17] Christensen RM. Yield and failure criteria for isotropic materials, http://www.failurecriteria.com/Media (2007; accessed on 14 December 2008).

[18] Prodromou, A. G., Lomov, S. V., & Verpoest, I. (2011). The method of cells and the mechanical properties of textile composites. *Composite structures*, *93*(4), 1290-1299.

[19] Falzon, P. J., & Herszberg, I. (1998). Mechanical performance of 2-D braided carbon/epoxy composites. *Composites science and technology*, *58*(2), 253-265.